The 22nd Conference of Mechanical Engineering Network of Thailand
15-17 October 2008, Thammasat University, Rangsit Campus, Pathum Thani, Thailand

Combined DKT Finite Element with Adaptive Meshing Technique for Plate Bending Analysis

Pichayen Bhothikhun[1] and Pramote Dechaumphai[2]*

[1,2]Department of Mechanical Engineering, Chulalongkorn University,
254 Phyathai Road, Patumwan, Bangkok 10330, Thailand,
*Tel: 0-2218-6621, Fax: 0-2218-6621 E-mail: fmepdc@eng.chula.ac.th

Abstract

An adaptive meshing technique is combined with the Discrete Kirchhoff Triangle (DKT) to analyze plate bending problems. The DKT plate bending finite element formulation with detailed finite element matrices are derived. An adaptive meshing technique is applied to generate small elements in the regions of high stress gradient to improve the computed solutions. Larger elements are generated in the other regions to reduce the problem unknowns and thus the computational time. The efficiency of the combined method is evaluated by several problems. Results show that the combined method can improve the solution accuracy and reduce the computational effort.

Keywords: finite element, adaptive mesh, plate bending, Discrete Kirchhoff Triangle

1. Introduction

The finite element method has been widely used for the analysis of plate bending problems. Different types of plate bending elements have been developed during the past decades. One of the element types which provide high solution accuracy for the analysis of plate bending, is the Discrete Kirchhoff Triangle (DKT) [1]. The three-node triangular DKT element is studied in this paper in order to combine with an adaptive meshing technique to improve the overall analysis solution accuracy. Detailed formulation and the corresponding finite element matrices of the DKT element are presented. The performance of the DKT element alone will be evaluated by a problem that has exact solution. The adaptive meshing technique presented herein generates small clustered elements in the regions of high stress gradients to provide higher solution accuracy. At the same time, larger elements are generated in the other regions to reduce the total number of unknowns and the computational time. Because the technique generates appropriate element sizes automatically, it is thus suitable for complex problems where a priori knowledge of the solutions does not exist. Herein, the technique has been combined with the DKT element for the analysis of plate bending in three-dimensional structures. Such structures are commonly modeled by using two-dimensional membrane and plate bending finite elements.

The governing differential equations for predicting the structural response due to mechanical load will be presented first. Then, the corresponding finite element equations and the associated element matrices will be derived and presented. The basic concepts of the adaptive meshing technique and the selection of the meshing parameters used for construction of new meshes will be explained. Finally, the performance of the DKT element and the adaptive meshing technique are evaluated by analyzing several examples.

2. Governing Equations

The equations for the in-plane deformation and the transverse deflection of a plate that lies in a local *x-y* coordinate system are briefly described herein.

2.1 In-Plane Deformation

The equations for the in-plane deformation are given by the two-dimensional equilibrium equations in the form

$$\frac{\partial \sigma_x}{\partial x} + \frac{\partial \tau_{xy}}{\partial y} + F_x = 0 \qquad (1)$$

$$\frac{\partial \tau_{xy}}{\partial x} + \frac{\partial \sigma_y}{\partial y} + F_y = 0 \qquad (2)$$

The stress components σ_x, σ_y and τ_{xy} are related to the strain components by the generalized Hooke's law as

$$\{\sigma\} = [C]\{\varepsilon\} \qquad (3)$$

where $\{\sigma\}$ contains the stress components σ_x, σ_y and τ_{xy}, and $[C]$ is the material stiffness matrix. For the plane stress case these material matrices are given in Ref. [2]. The vector of the strain components is related to the displacement gradients given by,

$$\{\varepsilon\}^T = \left\lfloor \frac{\partial u}{\partial x} \quad \frac{\partial v}{\partial y} \quad \frac{\partial u}{\partial y} + \frac{\partial v}{\partial x} \right\rfloor \qquad (4)$$

2.2 Transverse Deflection

The equation for the transverse deflection, *w*, in the *z*-direction normal to the *x-y* plane of a thin plate, is given by the equilibrium equation [3] as,

$$D\left(\frac{\partial^4 w}{\partial x^4}+\frac{\partial^4 w}{\partial x^2 \partial y^2}+\frac{\partial^4 w}{\partial y^4}\right) = p(x,y) \tag{5}$$

where $p(x,y)$ is the applied lateral load normal to the plate and D is the bending rigidity. The bending rigidity is defined by,

$$D = \frac{Et^3}{12(1-\nu^2)} \tag{6}$$

where E is the modulus of elasticity, t is the thickness of the plate and ν is the Poisson's ratio.

3. Derivation of Finite Element Equations

The constant strain triangle (CST) and the Discrete Kirchoff Triangle (DKT) finite elements are used for the in-plane deformation and the transverse deflection, respectively.

3.1 Constant Strain Triangle (CST)

The three-node CST element assumes a linear displacement distribution over the element. The element equations can be derived by applying the method of weighted residuals to the governing differential equations, Eq. (1) and (2), which leads to the element equations in the form of,

$$[K_m]\{\delta_m\} = \{F\} \tag{7}$$

where the vector $\{\delta_m\}$ contains the element nodal unknowns of the in-plane displacements in the element local *x-y* coordinate directions. There are two in-plane displacements per nodes or six unknowns per element. The element stiffness matrix, $[K_m]$, that appears in Eq. (7) is defined by Eq. (8).

$$[K_m] = [B_m]^T [C][B_m]tA \tag{8}$$

where the strain-displacement interpolation matrix, $[B_m]$, is given in Ref. [2]. The vector $\{F\}$ on the right-hand-side of Eq. (7) contains the applied mechanical forces at element nodes.

3.2 Discrete Kirchoff Triangle (DKT)

The three-node DKT element assumes a cubic distribution of the transverse deflection over the element [1]. The element equations can be derived by applying the method of weighted residuals to the plate bending equations, Eq. (5), which leads to the element equations in the form,

$$[K_b]\{\delta_b\} = \{F_p\} \tag{9}$$

where the vector $\{\delta_b\}$ contains the element nodal unknowns of the transverse deflections and the rotations. Each node has a transverse deflection in the element local *z*-coordinate direction and two rotations about the element local *x-y* coordinate directions. Thus there are nine degrees of freedom per element. The element stiffness matrix, $[K_b]$, and the nodal force vector due to the applied loads, $\{F_p\}$, are defined by,

$$[K_b] = \int_A [B_b]^T [D][B_b]\, dA \tag{10}$$

$$\{F_p\} = \int_A [N]^T p\, dA \tag{11}$$

where the strain-displacement interpolation matrix, $[B_b]$, is defined by,

$$[B_b]=\frac{1}{2A}\begin{bmatrix} y_{31}\left[\frac{\partial H_x}{\partial \xi}\right]+y_{12}\left[\frac{\partial H_x}{\partial \eta}\right] \\ -x_{31}\left[\frac{\partial H_y}{\partial \xi}\right]-x_{12}\left[\frac{\partial H_y}{\partial \eta}\right] \\ -x_{31}\left[\frac{\partial H_x}{\partial \xi}\right]-x_{12}\left[\frac{\partial H_x}{\partial \eta}\right]+y_{31}\left[\frac{\partial H_y}{\partial \xi}\right]+y_{12}\left[\frac{\partial H_y}{\partial \eta}\right] \end{bmatrix} \tag{12}$$

where

$$\left\{\frac{\partial H_x}{\partial \xi}\right\}=\begin{Bmatrix} P_6(1-2\xi)+\eta(P_5-P_6) \\ q_6(1-2\xi)-\eta(q_5+q_6) \\ -4+6(\xi+\eta)+r_6(1-2\xi)-\eta(r_5+r_6) \\ -P_6(1-2\xi)+\eta(P_4+P_6) \\ q_6(1-2\xi)+\eta(q_4-q_6) \\ -2+6\xi+r_6(1-2\xi)+\eta(r_4-r_6) \\ -\eta(P_4+P_5) \\ \eta(q_4-q_5) \\ \eta(r_4-r_5) \end{Bmatrix} \tag{13}$$

$$\left\{\frac{\partial H_y}{\partial \xi}\right\}=\begin{Bmatrix} t_6(1-2\xi)+\eta(t_5-t_6) \\ 1+r_6(1-2\xi)-\eta(r_5+r_6) \\ -q_6(1-2\xi)+\eta(q_5+q_6) \\ -t_6(1-2\xi)+\eta(t_4+t_6) \\ -1+r_6(1-2\xi)+\eta(r_4-r_6) \\ -q_6(1-2\xi)-\eta(q_4-q_6) \\ -\eta(t_4+t_5) \\ \eta(r_4-r_5) \\ -\eta(q_4-q_5) \end{Bmatrix} \tag{14}$$

$$\left\{\frac{\partial H_x}{\partial \eta}\right\}=\begin{Bmatrix} -P_5(1-2\eta)+\xi(P_5-P_6) \\ q_5(1-2\eta)-\xi(q_5+q_6) \\ -4+6(\xi+\eta)+r_5(1-2\eta)-\xi(r_5+r_6) \\ \xi(P_4+P_6) \\ \xi(q_4-q_6) \\ \xi(r_4-r_6) \\ P_5(1-2\eta)-\xi(P_4+P_5) \\ q_5(1-2\eta)+\xi(q_4-q_5) \\ -2+6\eta+r_5(1-2\eta)+\xi(r_4-r_5) \end{Bmatrix} \tag{15}$$

$$\left\{\frac{\partial H_y}{\partial \eta}\right\} = \left\{\begin{array}{c} -t_5(1-2\eta)+\xi(t_5-t_6) \\ 1+r_5(1-2\eta)-\xi(r_5+r_6) \\ -q_5(1-2\eta)+\xi(q_5+q_6) \\ \xi(t_4+t_6) \\ \xi(r_4-r_6) \\ -\xi(q_4-q_6) \\ t_5(1-2\eta)-\xi(t_4+t_5) \\ -1+r_5(1-2\eta)+\xi(r_4-r_5) \\ -q_5(1-2\eta)-\xi(q_4-q_5) \end{array}\right\} \qquad (16)$$

The coefficients P_k, q_k, r_k and t_k, k = 4, 5, 6 depend on the element shape and are given by,

$$P_k = \frac{-6x_{ij}}{\ell_{ij}^2} \quad (17) \; ; \quad q_k = \frac{3x_{ij}y_{ij}}{\ell_{ij}^2} \quad (18)$$

$$r_k = \frac{3y_{ij}^2}{\ell_{ij}^2} \quad (19) \; ; \quad t_k = \frac{-6y_{ij}}{\ell_{ij}^2} \quad (20)$$

$$\ell_{ij} = \sqrt{x_{ij}^2 + y_{ij}^2} \qquad (21)$$

where the coefficients x_{ij} and y_{ij}, $i, j = 1,\ 2,\ 3$ are defined in terms of element nodal coordinates by,

$$x_{ij} = x_i - x_j \quad (22) \; ; \quad y_{ij} = y_i - y_j \quad (23)$$

The matrix $[D]$ in Eq. (10) is the plate material stiffness matrix defined by,

$$[D] = \frac{Et^3}{12(1-\nu^2)}\begin{bmatrix} 1 & \nu & 0 \\ \nu & 1 & 0 \\ 0 & 0 & \frac{1-\nu}{2} \end{bmatrix} \qquad (24)$$

The above finite element matrices are in closed-form so that they can be implemented in the computer program directly [4].

4. Adaptive Meshing Technique

4.1 Adaptive Meshing concept

The basic idea of adaptive meshing [5] is to construct a completely new mesh based on the solution obtained from the previous mesh. The new mesh will have small elements in regions of large changes in solution gradients and large elements in regions where the gradient changes are small. Proper nodal spacings used for constructing a new mesh are determined by using the solid mechanics concept of finding the principal stresses, σ_1 and σ_2, from a given state of stresses, σ_x, σ_y and τ_{xy}, i.e.,

$$\begin{bmatrix} \sigma_x & \tau_{xy} \\ \tau_{xy} & \sigma_y \end{bmatrix} \Rightarrow \begin{bmatrix} \sigma_1 & 0 \\ 0 & \sigma_2 \end{bmatrix} \qquad (25)$$

At a typical node in the previous mesh, the second derivatives of the key parameter for meshing, ϕ, (analogous to the stress components in Eq. (25)) are computed and the two eigenvalues (analogous to the principal stresses) are then determined,

$$\begin{bmatrix} \frac{\partial^2\phi}{\partial x^2} & \frac{\partial^2\phi}{\partial x\partial y} \\ \frac{\partial^2\phi}{\partial x\partial y} & \frac{\partial^2\phi}{\partial y^2} \end{bmatrix} \Rightarrow \begin{bmatrix} \lambda_1 & 0 \\ 0 & \lambda_2 \end{bmatrix} \qquad (26)$$

The larger eigenvalue, $\lambda = \max(\lambda_1, \lambda_2)$, is then selected for that node and the same process is repeated for all the other nodes. Proper nodal spacings, denoted by h, used for constructing a new mesh are then determined from the condition required to procedure an optimal mesh;

$$\lambda h^2 = \text{constant} = \lambda_{\max} h_{\min}^2 \qquad (27)$$

where $\lambda_{\max}$ is the largest eigenvalue of all nodes in the previous mesh and $h_{\min}$ is the specified minimum nodal spacing for the new mesh.

4.2 Meshing Parameters

The adaptive meshing technique requires a selection of proper key parameters (ϕ in Eq. (26)). For structural problems under mechanical load, stress is an appropriate choice. However, the key parameter representing the stress should be a scalar quantity (directionally independent) such as the Von Mises stress defined in two dimensions by,

$$\sigma_{Von\ Mises} = \frac{1}{\sqrt{2}}\sqrt{(\sigma_x - \sigma_y)^2 + \sigma_x^2 + \sigma_y^2 + 6\tau_{xy}^2} \qquad (28)$$

For plate bending analysis, the Von Mises stress is used as a key parameter for meshing simultaneously so that the new mesh can capture the high stress concentration.

5. Applications

Three example problems are presented in this section. The first example is chosen to evaluate the performance of the DKT plate bending element. The second example demonstrates the effectiveness of the adaptive meshing technique combining with the DKT element. The third example combines both the CST and DKT elements, and demonstrates the capability of the adaptive meshing technique for 3D plate structures.

5.1 Partially loaded simply supported square plate

A square 2×2 m simply supported plate with a thickness of 0.01 m, subjected to a partially distributed load of 1 kN/m^2, is shown in Fig. 1. The plate is assumed to have the modulus of elasticity of 7.2×10^{10} N/m^2 and the Poisson's ratio of 0.25. The exact transverse deflection can be derived [3] and is given by,

$$w = \frac{4pa^4}{D\pi^5}\sum_{m=1,3,5,\ldots}^{\infty}\frac{(-1)^{(m-1)/2}}{m^5}\sin\frac{m\pi u}{2a}\left\{1 - \frac{\cosh\frac{m\pi y}{a}}{\cosh\alpha_m}\left[\cosh(\alpha_m - 2\gamma_m) + \gamma_m\sinh(\alpha_m - 2\gamma_m) + \alpha_m\frac{\sinh 2\gamma_m}{2\cosh\alpha_m}\right] + \frac{\cosh(\alpha_m - 2\gamma_m)}{2\cosh\alpha_m}\frac{m\pi y}{a}\sinh\frac{m\pi y}{a}\right\}\sin\frac{m\pi x}{a} \qquad (29)$$

Due to symmetry, a quarter of the plate is analyzed. The result of the transverse deflection obtained from the DKT element is shown in Fig. 2. Figure 3 shows the predicted transverse deflections along the x-direction obtained from the DKT element as compared to the exact solution. The figure shows good comparison of the two solutions.

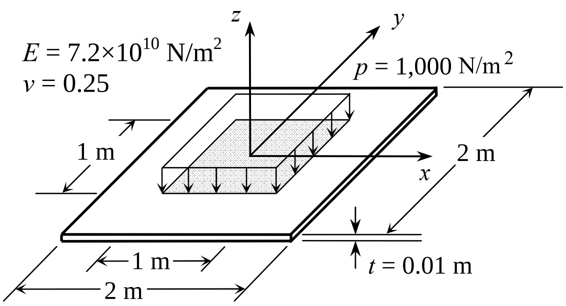

Figure 1. Problem statement of a simply supported square plate subjected to a partially distributed load.

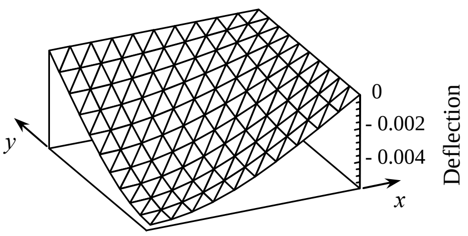

Figure 2. Predicted deflection of the plate using DKT plate bending element.

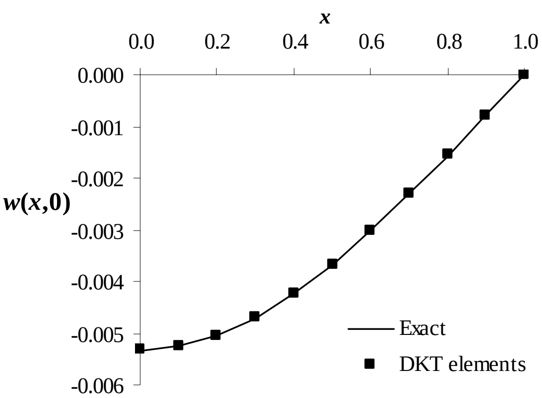

Figure 3. Comparative transverse deflections from DKT finite element model with the exact solution along x-direction for a simply supported square plate under partially distributed load.

5.2 Plate with narrow cut subjected to vertical loading

The problem statement of the plate with narrow cut subjected to vertical loading is shown in Fig. 4. The plate is subjected to the uniform vertical load p = 1 kN/m along one edge of the plate. The initial unstructured mesh consists of 299 nodes and 543 elements as shown in Fig. 5(a). The Von Mises stresses obtained from this initial mesh solution are used as the key parameter for the adaptive remeshing. The new adaptive mesh, with 849 nodes and 1604 elements, is shown in Fig. 5(b). Small elements are generated to concentrate in the region of high stress gradients near the end of the cutout to provide a more accurate stress solution. The second adaptive mesh with 1493 nodes and 2846 elements and the third adaptive mesh with 1953 nodes and 3734 elements are shown in Fig. 5(c) and 5(d) respectively. The figures show more refined elements are created in that region to capture the high stress concentration in order to increase the solution accuracy. Figure 6 shows that the predicted maximum Von Mises stress converges to the value of 2.40 GPa with the increase of the refined elements in the high stress concentration region. The deflection of the plate and the Von Mises stress contours by using the third adaptive finite element mesh are also shown in Fig. 7 and Fig. 8 respectively. Details of the Von Mises stress contours near the intense stress location are presented in Fig. 9.

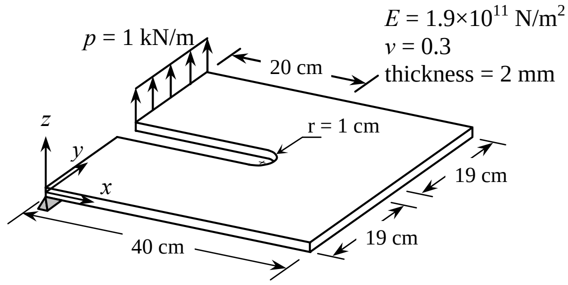

Figure 4. Problem statement of a plate with narrow cut subjected to vertical loading.

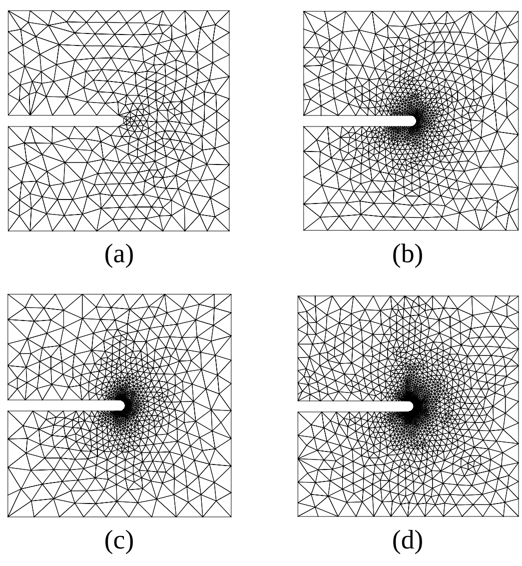

Figure 5. Unstructured DKT finite element meshes: (a) initial mesh, (b) 1st adaptive mesh, (c) 2nd adaptive mesh, and (d) 3rd adaptive mesh.

It is important to note that the adaptive meshing technique automatically generates refined elements in the region of high stresses. A priori knowledge of the solution to the problem is not needed before performing the analysis. The technique thus provides an advantage over the standard finite element procedure especially for more complex problems, such as the structure which will be presented in next example, where a priori knowledge of the solution does not exist.

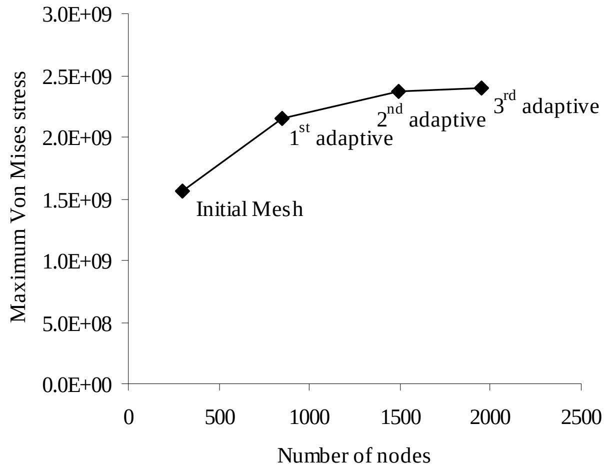

Figure 6. The convergence of predicted maximum Von Mises stress by using DKT adaptive finite element mesh.

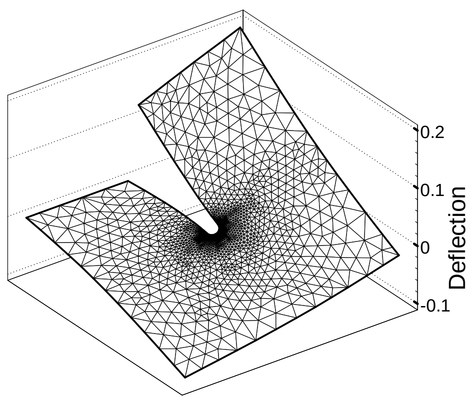

Figure 7. Predicted deflection of the plate using DKT 3rd adaptive finite element mesh.

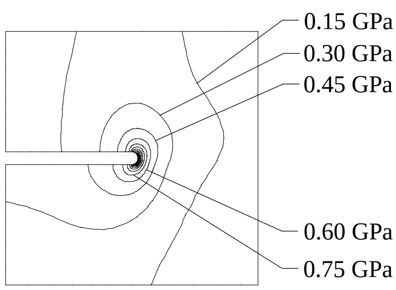

Figure 8. Predicted Von Mises stress contours of the plate using DKT 3rd adaptive finite element mesh.

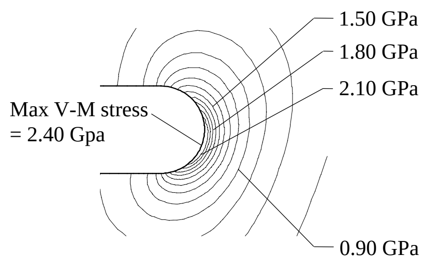

Figure 9. Predicted Von Mises stress contours of the plate using DKT 3rd adaptive finite element mesh in the region of high stresses.

5.3 Plate attached with roof-like section subjected to vertical loading

To demonstrate the capability of the adaptive meshing technique for stress analysis of more complex plate structures, a plate attached with roof-like section subjected to vertical loading is considered. A problem statement of this example is presented in Fig. 10. The square plate is clamped along the edge x=0 and subjected to the uniform vertical load along the opposite edge.

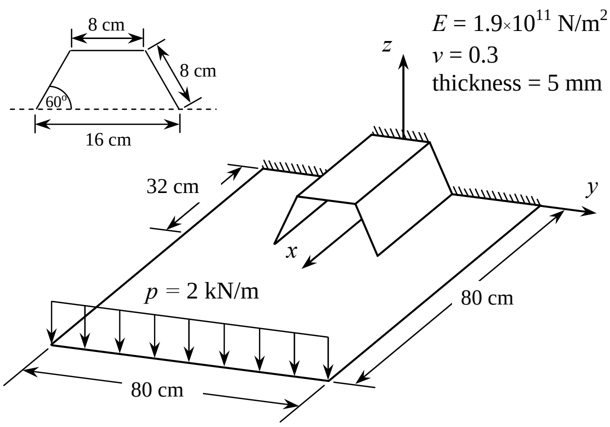

Figure 10. Problem statement of a plate attached with roof-like section subjected to the uniform vertical load.

Due to symmetry, the right half of the plate is analyzed. The initial unstructured coarse mesh consists of 264 nodes and 458 elements as shown in Fig. 11. The predicted Von Mises stress contours of the initial mesh are shown in Fig. 12. With these stresses, the new adaptive mesh with 865 nodes and 1645 elements shown in Fig. 13 is constructed. Small elements are generated to concentrate in the high stress regions at the corner of the intersection between the square plate and the roof-like section, while larger elements are generated in the other regions. The new refined mesh provides a more accurate and smooth stress distribution solution as shown in Fig. 14. The deflection of the new mesh of the plate is also shown in Fig. 15.

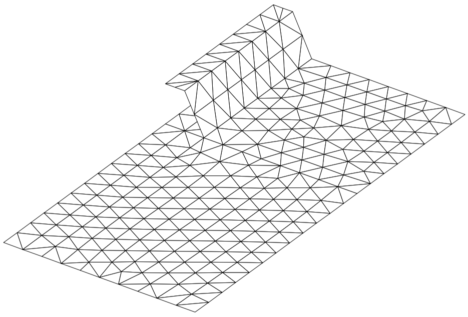

Figure 11. Initial finite element mesh of the plate attached with roof-like section.

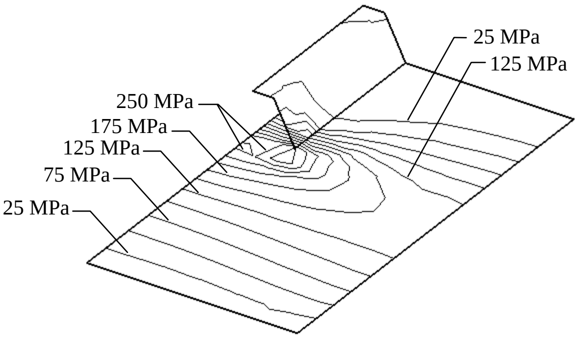

Figure 12. Predicted Von Mises stress contours of the plate attached with roof-like section using initial finite element mesh.

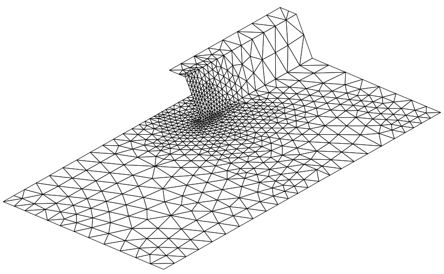

Figure 13. Adaptive finite element mesh of the plate attached with roof-like section with 865 nodes and 1645 elements.

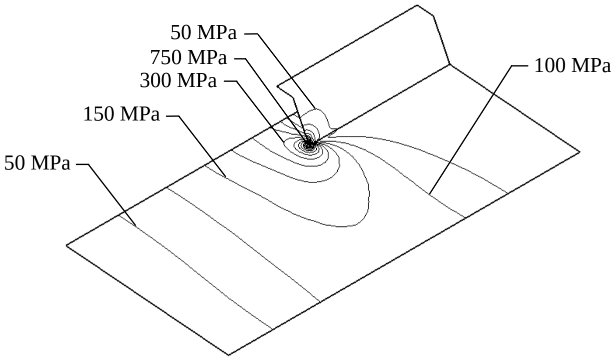

Figure 14. Predicted Von Mises stress contours of the plate attached with roof-like section using adaptive finite element mesh.

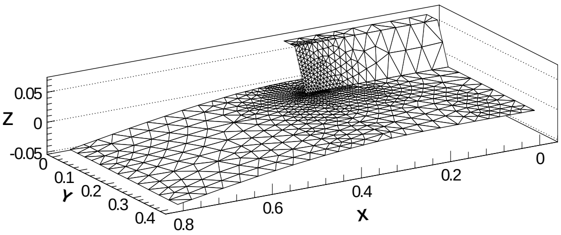

Figure 15. Predicted deflection of the plate attached with roof-like section using adaptive finite element mesh.

6. Conclusion

An adaptive meshing technique combined with the DKT finite element for plate bending analysis was presented. The DKT plate bending element has been combined with the adaptive meshing technique to improve the solution accuracy and reduce the computational effort. The examples presented in this paper demonstrated that the adaptive meshing technique: (1) reduces modeling effort because a priori knowledge of the solution is not required; (2) provides improved solution accuracy by adapting the mesh to the physics of the solutions; (3) reduces the total number of elements used in the finite element modeling by automatically generating small elements in the regions with high solution gradients and large elements in the other regions.

Acknowledgments

The authors are pleased to acknowledge the Thailand Research Fund (TRF) for supporting this research work.

References

[1] Batoz, J. L., Bathe, K. J., and Ho, L. W., 1980. A Study of Three-Node Triangular Plate Bending Elements. International Journal for Numerical Methods in Engineering, Vol. 15, pp. 1771-1812.

[2] Dechaumphai, P., 2007. Finite Element Method in Engineering. 4th Ed., Chulalongkorn University Press, Bangkok.

[3] Timoshenko, S. and Krieger, S. W., 1970. Theory of Plates and Shells. 3rd Ed., McGraw-Hill, Singapore.

[4] Jeyachandrabose, C., Kirkhope, J. and Babu, C. R., 1985. An Alternative Explicit Formulation for the DKT Plate-Bending Element, International Journal for Numerical Methods in Engineering, Vol. 21, pp. 1289-1293.

[5] Dechaumphai, P., 1996. Improvement of Plane Stress Solutions Using Adaptive Finite Elements. Journal of the Chinese Institute of Engineers, Vol. 19, No. 3, pp.375-380.